Multiple intersection exponents for planar Brownian motion

Achim Klenke
Johannes Gutenberg-Universität Mainz
Institut für Mathematik
Staudingerweg 9
55099 Mainz
Germany
math@aklenke.de
http://www.aklenke.de
Tel. +49+6131+3922829
Fax +49+6131+3920916

Peter Mörters
University of Bath
Department of Mathematical Sciences
Claverton Down
Bath BA2 7AY
United Kingdom
maspm@bath.ac.uk
http://www.bath.ac.uk/∼maspm

November 29th, 2008, revised June 1st, 2009

Abstract

Let $p \geq 2$, $n_1 \leq \cdots \leq n_p$ be positive integers and $B_1^1, \ldots, B_{n_1}^1; \ldots; B_1^p, \ldots, B_{n_p}^p$ be independent planar Brownian motions started uniformly on the boundary of the unit circle. We define a p-fold intersection exponent $\varsigma_p(n_1, \ldots, n_p)$, as the exponential rate of decay of the probability that the packets $\bigcup_{j=1}^{n_i} B_j^i[0, t^2]$, $i = 1, \ldots, p$, have no joint intersection. The case $p = 2$ is well-known and, following two decades of numerical and mathematical activity, Lawler, Schramm and Werner (2001) rigorously identified precise values for these exponents. The exponents have not been investigated so far for $p > 2$. We present an extensive mathematical and numerical study, leading to an exact formula in the case $n_1 = 1$, $n_2 = 2$, and several interesting conjectures for other cases.

AMS 2000 subject classification: 60J65.
Keywords: Brownian motion, intersection exponent.

1 Introduction

1.1 Motivation and overview

Finding *exponents*, which describe the decay of some probabilities, and *dimensions* of some sets associated with stochastic models of physical systems is one of the core activities in statistical physics. While in general one often has to resort to numerical methods to get a handle on the values of the exponents, for planar models conformal invariance may help to answer these questions explicitly, and there is now a substantial body of rigorous and non-rigorous methods available. For example, by making the assumption that critical planar percolation behaves in a conformally invariant way in the scaling limit and using ideas involving conformal field theory, Cardy [4] determined the asymptotic probability, as $N \to \infty$, that there exists a two-dimensional critical percolation cluster crossing a rectangle. A rigorous proof of Cardy's formula was later given by Smirnov [25]. Following considerable numerical work, see for example [18, 26] and references therein, Saleur and Duplantier [24] predicted the fractal dimension of the hull of a large percolation cluster using a non-rigorous Coulomb gas technique. Rigorous versions of this result have been given based on Cardy's formula, for example by Camia and Newman [2, 3].

In [6] Duplantier and Kwon suggested that ideas of conformal field theory can also be used to predict the probability of pairwise non-intersection between planar Brownian paths. Early research by Burdzy, Lawler and Polaski [1] and Li and Sokal [20] was of numerical nature, but ten years later, Duplantier [5] gave a derivation based on non-rigorous methods of quantum gravity, and soon after that Lawler, Schramm and Werner [14, 15, 16] gave a rigorous proof based on the Schramm-Loewner evolution (SLE), one of the greatest achievements in probability in recent years. We also mention here some very recent developments with the long term aim of making the quantum gravity approach rigorous, see Duplantier and Sheffield [7], and Rhodes and Vargas [23].

In this paper we look at joint intersections of three or more planar Brownian paths, a question which has been neglected so far in the literature, but which came up in our recent investigation of the multifractality of intersection local times [8]. In the simplest case, given three independent Brownian paths B^1, B^2, B^3 started uniformly on the unit circle, we are interested in the asymptotic behaviour, as $t \to \infty$, of the non-intersection probability

$$\mathbb{P}\big\{B^1[0,t] \cap B^2[0,t] \cap B^3[0,t] = \emptyset\big\}.$$

Observe that this probability goes to zero, for $t \uparrow \infty$, as three, or any finite number, of Brownian paths in the plane eventually intersect, see e.g. [21, Chapter 9.1]. Recall for comparison, that the non-intersection exponents for three Brownian paths studied in the aforementioned papers deal with pairwise non-intersections, i.e. in the case of three Brownian motions either with

$$\mathbb{P}\big\{B^1[0,t] \cap B^2[0,t] = \emptyset,\, B^2[0,t] \cap B^3[0,t] = \emptyset,\, B^1[0,t] \cap B^3[0,t] = \emptyset\big\}, \quad \text{or with}$$

$$\mathbb{P}\big\{B^1[0,t] \cap \big(B^2[0,t] \cup B^3[0,t]\big) = \emptyset\big\}.$$

Our study starts with the observation that, for positive integers $n_1, \ldots, n_p$ and independent planar Brownian motions

$$B^1_1, \ldots, B^1_{n_1}; \ldots; B^p_1, \ldots, B^p_{n_p},$$

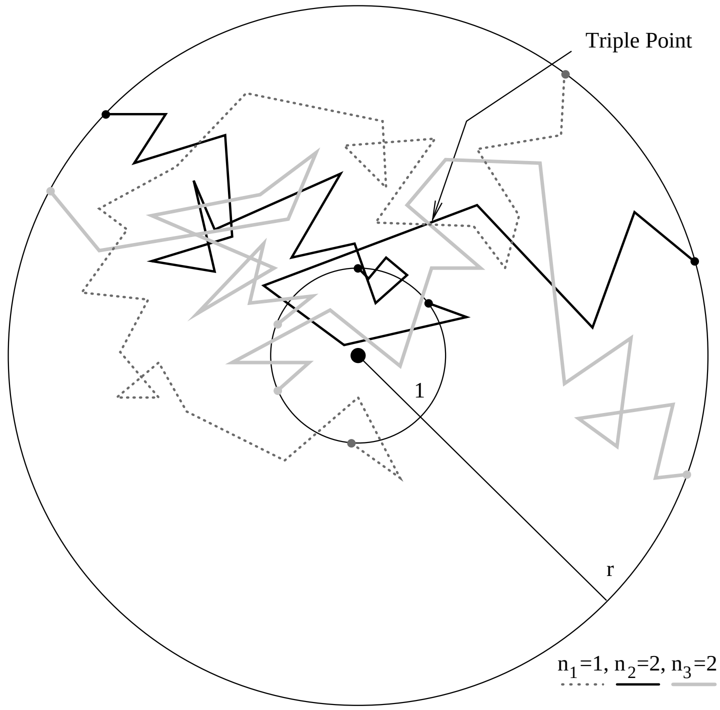

Figure 1: Illustration of a triple point ($p = 3$) with $n_1 = 1$, $n_2 = 2$ and $n_3 = 2$.

nontrivial exponents

$$\varsigma_p(n_1, \ldots, n_p) = - \lim_{t\to\infty} \frac{2}{\log t} \log \mathbb{P}\Big\{ \bigcup_{j=1}^{n_1} B_j^1[0,t] \cap \ldots \cap \bigcup_{j=1}^{n_p} B_j^p[0,t] = \emptyset \Big\}$$

exist, see Theorem 1 and the subsequent remark. In Theorem 2 we show that, for $2 \le n_3 \le \cdots \le n_p$, we have

$$\varsigma_p(1, 2, n_3, \ldots, n_p) = 2.$$

These are the only exponents we could determine exactly beyond the well-known case of $p = 2$. Rigorous proofs of both theorems are given in Section 2.

The bulk of this paper is devoted to the presentation of a detailed numerical study of the values of the, in our opinion, most interesting remaining exponents, see Section 3. One of the motivations of this study was to test the conjecture, motivated by Theorem 2, that the value of the exponents $\varsigma_p(n_1, n_2, n_3, \ldots, n_p)$ depend only on the two smallest parameters. This conjecture was not supported by our numerical investigations.

Finally, we remark that we have not been able to use either SLE techniques or quantum gravity to derive even a non-rigorous exact prediction of the exponents if $p > 2$. We hope however that our numerical study triggers interest in this problem and that, as in the motivational examples discussed above, future research will address the question of exact formulas for multiple intersection exponents.

1.2 Statement of the main theorems

Let $p \geq 2$ and $n_1, \ldots, n_p$ be positive integers and $B_1^1, \ldots, B_{n_1}^1; \ldots; B_1^p, \ldots, B_{n_p}^p$ independent planar Brownian motions started uniformly on the unit circle $\partial\mathcal{B}(0,1)$. We define p packets by

$$\mathfrak{B}^1(r) := \bigcup_{j=1}^{n_1} B_j^1\big[0, \tau_j^1(r)\big], \ldots, \mathfrak{B}^p(r) := \bigcup_{j=1}^{n_p} B_j^p\big[0, \tau_j^p(r)\big],$$

where $\tau_j^i(r) := \inf\{t \geq 0 \colon |B_j^i(t)| = r\}$ and $r \geq 1$.

Theorem 1. *The limit*

$$\varsigma_p(n_1, \ldots, n_p) := -\lim_{r \to \infty} \frac{1}{-\log r} \log \mathbb{P}\Big\{\mathfrak{B}^1(r) \cap \ldots \cap \mathfrak{B}^p(r) = \emptyset\Big\}$$

exists and is positive and finite.

Remarks:

- Using a standard argument, see [13, Lemma 3.14], one can replace the paths stopped upon hitting the circle of radius r, by paths running for $t = r^2$ time units. This leads to the characterisation of the exponents given in the overview.

- For $p = 2$ all exponents are known, see [14, 15, 16]:

  $$\varsigma_2(n_1, n_2) = \frac{\big(\sqrt{24n_1 + 1} + \sqrt{24n_2 + 1} - 2\big)^2 - 4}{48}.$$

  The technique used to identify the exponents, which is based on the Schramm-Loewner evolution (SLE), does not seem to allow us to identify the exponents for $p > 2$.

- We conjecture that one can strengthen this result, as this was done for $p = 2$ in [12], and show that there exists a constant $c > 0$, depending on the starting points, such that

  $$\lim_{r \to \infty} r^{\varsigma_p(n_1, \ldots, n_p)} \, \mathbb{P}\Big\{\mathfrak{B}^1(r) \cap \ldots \cap \mathfrak{B}^p(r) = \emptyset\Big\} = c.$$

  However, this is quite subtle and would go beyond the scope of this paper.

There is a trivial symmetry of the exponents, namely for every permutation $\sigma \in \mathrm{Sym}(p)$, we have

$$\varsigma_p\big(n_1, \ldots, n_p\big) = \varsigma_p\big(n_{\sigma(1)}, \ldots, n_{\sigma(p)}\big).$$

Moreover, there are two trivial monotonicity rules for these exponents

(A) $\varsigma_p(n_1, \ldots, n_p) \leq \varsigma_{p-1}(n_1, \ldots, n_{p-1})$,

(B) $\varsigma_p(n_1, \ldots, n_p) \leq \varsigma_p(m_1, \ldots, m_p)$, if $n_i \leq m_i$ for $i = 1, \ldots, p$.

As a result of the symmetry of the exponents, we may henceforth assume that the arguments of the exponents are increasing in size, i.e. $n_1 \le \cdots \le n_p$. There is one interesting situation in which we can determine the exponents explicitly.

Theorem 2. *We have* $\varsigma_p(1,2,n_3,\dots,n_p) = 2$ *for any* $p \ge 2$ *and* $2 \le n_3 \le \cdots \le n_p$.

As $\varsigma_p(1,2,\dots,2) \le \varsigma_p(1,2,n_3,\dots,n_p) \le \varsigma_2(1,2)$ by the monotonicity rules, it suffices to show that

$$\varsigma_p(1,2,\dots,2) = 2\,. \tag{1.1}$$

The proof of this fact is based on the technique of hitting the intersection of $p-1$ Brownian paths by a further path, using an idea of Lawler, see [10] or [11, Section 3], originally used to determine the exponent $\varsigma_2(1,2) = 2$.

Remark: The definition of the exponents $\varsigma_p(n_1,\dots,n_p)$ can be naturally extended to a *real* argument $\lambda > 0$ in place of n_p by letting

$$\begin{aligned}&\varsigma_p(n_1,\dots,n_{p-1},\lambda) := \\ &\quad -\lim_{r\to\infty} \frac{1}{-\log r} \log \mathbb{E}\Big[\mathbb{P}\big\{\mathfrak{B}^1(r) \cap \ldots \cap \mathfrak{B}^{p-1}(r) \cap B_1^p\big[0,\tau_1^p(r)\big] = \emptyset \,\big|\, \mathfrak{B}^1(r),\dots,\mathfrak{B}^{p-1}(r)\big\}^\lambda\Big].\end{aligned}$$

The mapping $\lambda \mapsto \varsigma_p(n_1,\dots,n_{p-1},\lambda)$ cannot always be analytic: for instance, recall that $\varsigma_3(1,2,1) \le \varsigma_2(1,1) = \frac{5}{4}$, but $\varsigma_3(1,2,\lambda) = 2$ for all $\lambda \ge 2$, by Theorem 2 and the monotonicity rules. However, for $p = 2$ this mapping is analytic, see [17].

1.3 Conjectures

In this section we formulate the main conjecture motivated by our numerical studies. A detailed description of these studies and their outcomes will be given in Section 3.

Let $p \in \mathbb{N}$ and $n_1,\dots,n_p \in \mathbb{N}$ with $n_1 \le n_2 \le \cdots \le n_p$. Define

$$k := \max\big\{2,\, \min\big\{\ell \in \{1,\dots,p\}\colon\ n_{\ell+1} > n_\ell\big\}\big\},$$

with $k := p$ if the set is empty. We conjecture that

$$\varsigma_p(n_1,\dots,n_p) = \varsigma_k(n_1,\dots,n_k). \tag{1.2}$$

In fact, this holds, by Theorem 2 for the case $k = 2$, $n_k = 2$, and we have numerical evidence for

- $\varsigma_3(1,1,2) = 1.2503 \pm 0.0011$ to be compared with $\varsigma_2(1,1) = \frac{5}{4}$
- $\varsigma_4(1,1,1,2) = 1.02 \pm 0.004$ to be compared with $\varsigma_3(1,1,1) = 1.027 \pm 0.005$
- $\varsigma_3(2,2,3) = 2.937 \pm 0.01$ to be compared with $\varsigma_2(2,2) = \frac{35}{12} = 2.91666\ldots$.

This is evidence that if p packets of Brownian motions are required not to intersect, this is achieved by the k smallest packets not intersecting, if these are *strictly* smaller than the $p-k$ largest packets. Beyond this conjecture it is interesting to compare further values, namely

- $\varsigma_3(1,3,3) = 2.688 \pm 0.01$ with $\varsigma_2(1,3) = \frac{13+\sqrt{73}}{8} = 2.693000\ldots$

- $\varsigma_3(2,3,3) = 3.767 \pm 0.06$ with $\varsigma_2(2,3) = \frac{47+5\sqrt{73}}{24} = 3.738334113\ldots$,

which is evidence supporting the conjecture that in some cases nonintersection is achieved by the two smallest packets not intersecting, even if the second and third smallest have the same size. However this cannot be expected in all situations, as can be seen comparing

- $\varsigma_3(1,1,1) = 1.027 \pm 0.005$ with $\varsigma_2(1,1) = \frac{5}{4}$.

2 Proofs of Theorems 1 and 2.

2.1 Proof of Theorem 1

Denote by $x = (x_1^1, \ldots, x_{n_1}^1; \ldots; x_1^p, \ldots, x_{n_p}^p)$ vectors with $n_1 + \cdots + n_p$ entries in $\mathbb{R}^2$, playing the role of configurations of our motions at time zero. Consider

$$a_r := \sup_{|x_j^i|=1} \mathbb{P}_x\big\{\mathfrak{B}^1(r) \cap \cdots \cap \mathfrak{B}^p(r) = \emptyset\big\},$$

where the subindex of $\mathbb{P}$ indicates the starting points of the Brownian motions. Using the strong Markov property and Brownian scaling, we get, for any $r, s \geq 1$,

$$\begin{aligned}
a_{rs} \leq & \sup_{|x_j^i|=1} \mathbb{P}_x\Big\{ \bigcup_{j=1}^{n_1} B_j^1\big[0, \tau_j^1(r)\big] \cap \cdots \cap \bigcup_{j=1}^{n_p} B_j^p\big[0, \tau_j^p(r)\big] = \emptyset, \\
& \qquad \bigcup_{j=1}^{n_1} B_j^1\big[\tau_j^1(r), \tau_j^1(rs)\big] \cap \cdots \cap \bigcup_{j=1}^{n_p} B_j^p\big[\tau_j^p(r), \tau_j^p(rs)\big] = \emptyset \Big\} \\
= & \sup_{|x_j^i|=1} \mathbb{E}_x\Big[1\Big\{ \bigcup_{j=1}^{n_1} B_j^1\big[0, \tau_j^1(r)\big] \cap \cdots \cap \bigcup_{j=1}^{n_p} B_j^p\big[0, \tau_j^p(r)\big] = \emptyset \Big\} \\
& \qquad \times \mathbb{P}_{(B_j^i(\tau_j^i(r)))}\Big\{ \bigcup_{j=1}^{n_1} B_j^1\big[\tau_j^1(r), \tau_j^1(rs)\big] \cap \cdots \cap \bigcup_{j=1}^{n_p} B_j^p\big[\tau_j^p(r), \tau_j^p(rs)\big] = \emptyset \Big\} \Big] \\
\leq & \, a_r a_s \,.
\end{aligned}$$

Hence the function given by $b_t := \log a_{2^t}$ is subadditive and, by the subadditivity lemma, see e.g. [11, Lemma 5.2.1], we thus have $\lim_{t\to\infty} b_t/t = \inf_{t>0} b_t/t$. Therefore,

$$\tilde{\varsigma}_p(n_1, \ldots, n_p) := -\lim_{r\to\infty} \frac{1}{\log r} \log \sup_{|x_j^i|=1} \mathbb{P}_x\big\{\mathfrak{B}^1(r) \cap \cdots \cap \mathfrak{B}^p(r) = \emptyset\big\}$$

exists, and is positive.

Next, we show that we can replace the optimised starting points by starting points uniformly chosen from the unit circle. Clearly, we have

$$\mathbb{P}\big\{\mathfrak{B}^1(r) \cap \cdots \cap \mathfrak{B}^p(r) = \emptyset\big\} \leq \sup_{|x_j^i|=1} \mathbb{P}_x\big\{\mathfrak{B}^1(r) \cap \cdots \cap \mathfrak{B}^p(r) = \emptyset\big\}, \tag{2.1}$$

where $\mathbb{P}$ refers to the original scenario of Brownian motions started uniformly on the unit circle.

Conversely, using the Markov property, for $r > 2$, we have

$$\sup_{|x_j^i|=1} \mathbb{P}_x\big\{\mathfrak{B}^1(r) \cap \cdots \cap \mathfrak{B}^p(r) = \emptyset\big\}$$
$$\leq \sup_{|x_j^i|=1} \mathbb{E}_x\Big[\mathbb{P}_{(B_j^i(\tau_j^i(2)))}\Big\{\bigcup_{j=1}^{n_1} B_j^1\big[\tau_j^1(2), \tau_j^1(r)\big] \cap \cdots \cap \bigcup_{j=1}^{n_p} B_j^p\big[\tau_j^p(2), \tau_j^p(r)\big] = \emptyset\Big\}\Big].$$

By the Harnack principle, the law of the vector $(B_j^i(\tau_j^i(2)))$ is bounded, uniformly in x, by a constant multiple of the uniform distribution on the $(n_1 + \cdots + n_p)$-fold cartesian power of the circle $\partial\mathcal{B}(0, 2)$. Denoting this constant by C and using Brownian scaling,

$$\begin{aligned} &\mathbb{P}\Big\{\bigcup_{j=1}^{n_1} B_j^1\big[0, \tau_j^1(r/2)\big] \cap \cdots \cap \bigcup_{j=1}^{n_p} B_j^p\big[0, \tau_j^p(r/2)\big] = \emptyset\Big\} \\ &\qquad \geq C^{-1} \sup_{|x_j^i|=1} \mathbb{P}_x\big\{\mathfrak{B}^1(r) \cap \cdots \cap \mathfrak{B}^p(r) = \emptyset\big\}. \end{aligned} \tag{2.2}$$

Combining (2.1) and (2.2) yields that

$$\varsigma_p(n_1, \ldots, n_p) := -\lim_{r\to\infty} \frac{1}{\log r} \log \mathbb{P}\big\{\mathfrak{B}^1(r) \cap \cdots \cap \mathfrak{B}^p(r) = \emptyset\big\}$$

exists and coincides with $\tilde{\varsigma}_p(n_1, \ldots, n_p)$. Note, finally, that the monotonicity rule (A) implies that $\varsigma_p(n_1, \ldots, n_p) \leq \varsigma_2(n_1, n_2) < \infty$, and hence the exponents are positive and finite. $\diamond$

2.2 Proof of Theorem 2

Recall that it suffices to show (1.1). We start by formulating the key lemma. We let $W^1, \ldots, W^p$ be independent Brownian paths. For $r, s > 0$ denote by $\tau^i(x, r)$ the first hitting time by the motion W^i of the circle $\partial\mathcal{B}(x, r)$ with centre x and radius r, and let $\tau^i(x, r, s)$ be the first hitting time of $\partial\mathcal{B}(x, s)$ after $\tau^i(x, r)$.

Lemma 3. *Fix $x \in \mathcal{B}(0, 1)$. Suppose that $W^1, \ldots, W^p$ are independent Brownian paths started uniformly on the circle $\partial\mathcal{B}(0, 2)$. Define the set*

$$\mathfrak{W} := \bigcap_{j=2}^{p} W^j[0, \tau^j(0, 4)] \tag{2.3}$$

and the events

$$\begin{aligned} E_{x,r} &= \big\{W^1[0, \tau^1(x, r/2)] \cap \mathfrak{W} = \emptyset\big\}, \\ N_{x,r} &= \big\{W^1[0, \tau^1(x, r/2, r)] \cap \mathfrak{W} \neq \emptyset\big\}, \\ H_{x,r} &= \big\{\tau^i(x, r/2) < \tau^i(0, 4) \ \textit{for all} \ i = 1, \ldots, p\big\}. \end{aligned} \tag{2.4}$$

Then

$$\liminf_{r\downarrow 0} \frac{1}{|\log r|} \log \mathbb{P}\big[E_{x,r} \cap N_{x,r} \,\big|\, H_{x,r}\big] \geq -\varsigma_p(1, 2, \ldots, 2).$$

Let us first see how (1.1) follows from this lemma. Let

$$\tau = \inf\big\{t > 0 \,:\, W^1(t) \in \mathfrak{W}\big\}.$$

Now let $\mathfrak{B}$ be a collection of pairwise disjoint discs of fixed radius $0 < r < 1/2$ with centres in the disc $\mathcal{B}(0,1)$, which has cardinality at least $(2r)^{-2}$. Then, obviously,

$$1 \;\geq\; \mathbb{P}\big\{W^1[0,\tau^1(0,4)] \cap \mathfrak{W} \neq \emptyset\big\} \;\geq\; \sum_{\mathcal{B}\in\mathfrak{B}} \mathbb{P}\big\{W^1(\tau) \in \mathcal{B},\, \tau < \tau^1(0,4)\big\}\,.$$

Now, fix a disc $\mathcal{B} = \mathcal{B}(x,r) \in \mathfrak{B}$. The event $\{W^1(\tau) \in \mathcal{B},\, \tau < \tau^1(0,4)\}$ is implied by the events

$$E_{x,r} \cap N_{x,r} \cap \{\tau^1(x,r/2) < \tau^1(0,4)\}.$$

Recall that

$$\mathbb{P}\big[H_{x,r}\big] = \mathbb{P}\big\{\tau^1(x,r/2) < \tau^1(0,4)\big\}^p = r^{o(1)}\,.$$

Combining this with Lemma 3, for any $\varepsilon > 0$ and sufficiently small $r > 0$,

$$\mathbb{P}\big\{W^1(\tau) \in \mathcal{B},\, \tau < \tau^1(0,4)\big\} \geq r^{\varsigma_p(1,2,\dots,2)+\varepsilon}.$$

This implies

$$1 \geq \sum_{\mathcal{B}\in\mathfrak{B}} r^{\varsigma_p(1,2,\dots,2)+\varepsilon} \geq r^{-2+\varsigma_p(1,2,\dots,2)+2\varepsilon}\,,$$

and therefore $\varsigma_p(1,2,\dots,2) \geq 2 - 2\varepsilon$. The lower bound follows as $\varepsilon > 0$ was arbitrary, and the upper bound in (1.1) follows from $\varsigma_p(1,2,\dots,2) \leq \varsigma_2(1,2) = 2$, as is known from [10, 11]. ⋄

Proof of Lemma 3. Before we describe the technical details we sketch the idea of the proof. Since the paths of p planar Brownian motions intersect with positive probability, by Brownian scaling, the conditional probability of $N_{x,r}$ given $H_{x,r}$ is bounded from below as $r \to 0$. Hence this condition can be neglected when computing the probability in Lemma 3. For $j = 1,\dots,p$ we decompose the paths W^j into the pieces $W^j[0,\tau^j(x,r/2)]$ and $W^j[\tau^j(x,r/2),\tau^j(0,4)]$. By time reversal for $W^j[0,\tau^j(x,r/2)]$, we can compare the probability in question with the non-intersection probability for packets of size $n_1 = 1$, $n_2 = \dots = n_p = 2$, which is of order $\approx r^{\varsigma_p(1,2,\dots,2)}$.

We now come to the technical details, see the appendix in [22] for the necessary facts about Brownian excursions between concentric spheres. Let $\varrho^1 = r$ and $\varrho^j = r/2$ for $j = 2,\dots,p$. Conditioned on $\{\tau^i(x,\varrho^j/2) < \tau^i(x,3)\}$ the path $W^i[0,\tau^i(x,\varrho^j/2)]$ is contained in an excursion from $\partial\mathcal{B}(x,3)$ to $\partial\mathcal{B}(x,\varrho^j/2)$. The time-reversal of this excursion is contained in the path of a Brownian motion $\widetilde{W}^i$ started uniformly on $\partial\mathcal{B}(x,\varrho^j/2)$ and stopped upon reaching $\partial\mathcal{B}(x,3)$, say at time $\widetilde{\tau}^i(x,3)$. Analogously to (2.3) and (2.4) define the set

$$\widetilde{\mathfrak{W}} = \bigcap_{j=2}^{p} \big(\widetilde{W}^j[0,\widetilde{\tau}^j(x,3)] \cup W^j[\tau^j(x,r/4,r/2),\tau^j(0,4)]\big),$$

and the events

$$\widetilde{E}_{x,r} = \big\{\widetilde{W}^1[0,\widetilde{\tau}^1(x,3)] \cap \widetilde{\mathfrak{W}} = \emptyset\big\},$$

$$\widetilde{N}_{x,r} = \Big\{\bigcap_{j=1}^{p} W^j[\tau^j(x,\rho^j/2),\tau^j(x,\rho^j/2,\rho^j)] \neq \emptyset\Big\},$$

$$\widetilde{H}_{x,r} = \big\{\tau^j(x,\varrho^j/2) < \tau^j(x,3) \;\text{ for all }\; j = 1,\dots,p\big\}.$$

Note that $W^1[0,\tau^1(x,\rho^1)] \cap \mathcal{B}(x,r/2) = \emptyset$ and $W^j[\tau^j(x,\rho^j/2), \tau^j(x,\rho^j/2,\rho^j)) \subset \mathcal{B}(x,r/2)$ for $j = 2,\dots,p$. Hence

$$W^1[0,\tau^1(x,\rho^1)] \cap \big(\mathfrak{W} \setminus \widetilde{\mathfrak{W}}\big) \subset W^1[0,\tau^1(x,\rho^1)] \cap \bigcap_{j=2}^{p} W^j[\tau^j(x,\rho^j/2), \tau^j(x,\rho^j/2,\rho^j)) = \emptyset$$

which implies $\widetilde{E}_{x,r} \subset E_{x,r}$. Note that trivially, we have $\widetilde{H}_{x,r} \subset H_{x,r}$ and $\widetilde{N}_{x,r} \subset N_{x,r}$ which implies

$$E_{x,r} \cap N_{x,r} \cap H_{x,r} \ \supset\ \widetilde{E}_{x,r} \cap \widetilde{N}_{x,r} \cap \widetilde{H}_{x,r}. \tag{2.5}$$

Finally, note that

$$f(x,r) := \frac{\mathbb{P}[\widetilde{H}_{x,r}]}{\mathbb{P}[H_{x,r}]} = \frac{\mathbb{P}\big\{\tau^1(x,\varrho^1/2) < \tau^1(x,3)\big\}^p}{\mathbb{P}\big\{\tau^1(x,r/2) < \tau^1(0,4)\big\}^p} \geq \frac{1}{2} \tag{2.6}$$

for all x and for sufficiently small values of $r > 0$.
By (2.5), (2.6) and the definition of the conditional probability, we conclude

$$\mathbb{P}\big[E_{x,r} \cap N_{x,r} \,\big|\, H_{x,r}\big] \geq f(x,r)\, \mathbb{P}\big[\widetilde{E}_{x,r} \cap \widetilde{N}_{x,r} \big| \widetilde{H}_{x,r}\big]. \tag{2.7}$$

Fix $\varepsilon > 0$. Invoking the definition of the exponent, the Harnack principle and Brownian scaling, for sufficiently small $r > 0$,

$$\mathbb{P}\big[\widetilde{E}_{x,r} \,\big|\, \widetilde{H}_{x,r}\big] \geq r^{\varsigma_p(1,2,\dots,2)+\varepsilon}.$$

Define the compact sets

$$C := \big\{y = (y^1,\dots,y^p) : y^j \in \partial\mathcal{B}(0,\varrho^j/2) \ \text{ for } j = 1,\dots,p\big\} \ \text{ and}$$
$$D := \big\{z = (z^1,\dots,z^p) : z^j \in \partial\mathcal{B}(0,\varrho^j) \ \text{ for } j = 1,\dots,p\big\}.$$

For $y \in C$ and $z \in D$ let $(\bar{W}^j,\ j = 1,\dots,p)$ be an independent family of Brownian motions where each motion $\bar{W}^j$ is started at y^j and is conditioned to leave $\mathcal{B}(0,\varrho^j)$ at z^j (at time $\bar{\tau}^j$). Denote by $\mathbb{P}_{y,z}$ the corresponding probability measure. It is easy to see that the map

$$\phi : C \times D \to [0,1], \quad (y,z) \mapsto \mathbb{P}_{y,z}\big\{\bar{W}^1[0,\tau^1] \cap \ldots \cap \bar{W}^p[0,\tau^p] \neq \emptyset\big\}$$

is continuous and strictly positive, and independent of r by Brownian scaling. Hence

$$c := \inf_{y \in C,\, z \in D} \phi(y,z) > 0.$$

We infer that

$$\mathbb{P}\big[\widetilde{N}_{x,r} \,\big|\, \widetilde{E}_{x,r} \cap \widetilde{H}_{x,r}\big] \geq c > 0.$$

Hence, combing our results, for sufficiently small $r > 0$

$$\mathbb{P}\big[\widetilde{E}_{x,r} \cap \widetilde{N}_{x,r} \big| \widetilde{H}_{x,r}\big] = \mathbb{P}\big[\widetilde{E}_{x,r} \,\big|\, \widetilde{H}_{x,r}\big] \mathbb{P}\big[\widetilde{N}_{x,r} \,\big|\, \widetilde{E}_{x,r} \cap \widetilde{H}_{x,r}\big] \geq c\, r^{\varsigma_p(1,2,\dots,2)+\varepsilon},$$

and this completes the proof as $\varepsilon > 0$ was arbitrary. ◇

3 Simulations

To get hold of those exponents which we could not determine explicitly, we have performed Monte Carlo simulations. This has successfully generated conjectures in the $p = 2$ case, see Duplantier and Kwon [6], Li and Sokal [20] and Burdzy, Lawler and Polaski [1].

3.1 The general scheme. Before we list and analyse the simulated data, we explain how we got it. Fix positive integers p and $n_1, \dots, n_p$. The aim is to get an estimate on $\varsigma_p(n_1, \dots, n_p)$. Instead of Brownian motions we simulate two-dimensional symmetric nearest neighbour random walks. As it reduces computing effort, we work with boxes rather than with discs. (For comparison we have performed some of the simulations also with discs and there was no significant difference in the results.) First we fix an increasing sequence of box half-lengths $L_0, \dots, L_K$ (in most cases $L_{k+1} = \lfloor 1.1 \cdot L_k \rfloor$ and the maximal value $m = L_L$ restricted to 20000, 40000 or 80000) and the sample size N of the simulation.

Step 1. We start $n_1 + \dots + n_p$ independent random walks at the origin $0 \in \mathbb{Z}^2$ and stop each of them when it hits the (graph) boundary of the box $\{-L_0, \dots, L_0\}^2 = [-L_0, L_0]^2 \cap \mathbb{Z}^2$. This defines the starting positions of the random walks.

Step 2. Assume we are at level k (after Step 1 we are at level $k = 1$). Independently run the random walks until they hit the boundary of the box $\{-L_k, \dots, L_k\}^2 \subset \mathbb{Z}^2$. Separately, keep track of the set $A_{k,i} \subset \{-L_k + 1, \dots, L_k - 1\}^2$ of points that are visited by the ith package of n_i random walks *before* hitting the boundary of $\{-L_k, \dots, L_k\}^2$ (after Step 1).

If $A_{k,1} \cap \dots \cap A_{k,p} = \emptyset$, then we say that we have *survived* level k and we enter level $k+1$ (that is, we perform Step 2 again with k replaced by $k+1$). Otherwise we stop this sample and start a new simulation in Step 1.

By N_k we denote the number of samples that have survived level k. Clearly, $N_0 = N$. We should have

$$N_k/N \approx (L_k/L_0)^{-\varsigma_p(n_1,\dots,n_p)}.$$

Hence in a double logarithmic plot of $\log(N_k)$ against $\log(L_k)$ the points should be on a line with slope $-\varsigma_p(n_1, \dots, n_p)$. Linear regression then gives an estimate for the exponent $\varsigma_p(n_1, \dots, n_p)$.

As it turns out that a line can be fitted well only for large values of L_k, we have neglected the small values of L_k in order to get a reasonable estimate for $\varsigma_p(n_1, \dots, n_p)$. In Figure 3.4.1 below we plotted the data points used for the linear regression with solid circles, the other points with hollow circles.

As can be seen from Figure 3.4.1, for $\xi(1,1)$ this gives a pretty good estimate of the exact value $\frac{5}{4}$, even with a moderate computing effort of about 2000 hours CPU time. However, for $\xi(1,1,1)$ the points tend to lie on a straight line only for large values of L_k and thus require

(i) a large maximal box size $m = L_K$ and thus a big computer memory of size $(2m+1)^2$ bytes in order to keep track of the visited points,

(ii) a large sample size N_0 in order that $N_K \approx N_0 \cdot (L_K/L_0)^{-\xi(1,1,1)}$ is big enough to obtain reliable data from the simulation.

Since the CPU time we need for each sample grows with m, (i) and (ii) imply that we need huge amounts of CPU time. Furthermore, with huge sample sizes and box sizes, we run into the order of the cycle length of the common 48 bit linear congruence random number generators.

The computations were performed on different computers, mainly on two parallel Linux clusters at the University of Mainz on Opteron 2218 processors with 2.6GHz and on Opteron 244 processors with 1.8GHz. The programme code is written in C. As random number generator we used `drand64()`, a 64 bit linear congruence generator following the rule

$$r_{n+1} = (ar_n + c) \mod 2^{64}$$

with

$$a = 6364136223846793005 \quad \text{and} \quad c = 1$$

(see [9, pp106-108]).

The linear regression method does not give a quantitative estimate on the statistical error. In order to get such an error estimate we did the following. Having in mind that the systematic error is large for small box sizes, we choose a minimal box number $k_{\min} \in \{1, \ldots, K-1\}$ and neglect the data from all smaller boxes. Furthermore, we pretend that the asymptotics for p_L is exact for $k \geq k_{\min}$, that is,

$$p_{L_k} = C\, L_k^{-\varsigma} \quad \text{for all } k \geq k_{\min} \tag{3.1}$$

for some $C > 0$. In particular, the conditional probability to have no multiple intersections before leaving $B_{L_{k+1}}$ given there is no multiple intersection before leaving B_{L_k} is

$$\bar{p}_k := \frac{p_{L_{k+1}}}{p_{L_k}} = \left(\frac{L_k}{L_{k+1}}\right)^{-\varsigma} =: q_k^{-\varsigma}.$$

Here the likelihood function for the observation

$$(N_{k_{\min}}, N_{k_{\min}+1}, \ldots, N_K) = n := (n_{k_{\min}}, n_{k_{\min}+1}, \ldots, n_K)$$

is

$$\begin{aligned} L_n(\varsigma) &= C(n) \prod_{l=k_{\min}}^{K-1} \bar{p}_l^{\,n_{l+1}} (1 - \bar{p}_l)^{n_l - n_{l+1}} \\ &= C(n) \prod_{l=k_{\min}}^{K-1} \bar{q}_l^{\,\varsigma n_{l+1}} (1 - \bar{q}_l^{\,\varsigma})^{n_l - n_{l+1}} \end{aligned} \tag{3.2}$$

for some $C(n) > 0$. The log-likelihood function is

$$\mathcal{L}_n(\varsigma) = \log C(n) + \sum_{l=k_{\min}}^{K-1} \Big(n_{l+1} \varsigma \log(q_l) \; + \; (n_l - n_{l+1}) \log\big(1 - q_l^{\varsigma}\big)\Big). \tag{3.3}$$

The maximum likelihood estimator (MLE) $\hat{\varsigma}$ is defined by

$$\mathcal{L}_n\big(\hat{\varsigma}\big) = \sup_{\varsigma > 0} \mathcal{L}_n(\varsigma). \tag{3.4}$$

We compute the derivatives

$$\mathcal{L}_n'(\varsigma) = \sum_{l=k_{\min}}^{K-1} n_{l+1} \log(q_l) \; - \; \sum_{l=k_{\min}}^{K-1} (n_l - n_{l+1}) \frac{\log(q_l)\, q_l^{\varsigma}}{1 - q_l^{\varsigma}} \tag{3.5}$$

and

$$\mathcal{L}_n''(\varsigma) = -\sum_{l=k_{\min}}^{K-1} (n_l - n_{l+1}) \frac{(\log(q_l))^2 \, q_l^{\varsigma}}{(1-q_l^{\varsigma})^2}. \tag{3.6}$$

Clearly, $\mathcal{L}_n''(\varsigma) < 0$, hence $\varsigma \mapsto \mathcal{L}_n(\varsigma)$ is strictly concave and thus $\hat{\varsigma}$ is the unique solution of

$$\mathcal{L}_n'(\hat{\varsigma}) = 0. \tag{3.7}$$

Hence, for given data, the MLE can easily be computed numerically (we used a Newton approximation scheme).

Denote by $\hat{\varsigma}_{n_0}$ the MLE for sample size n_0. By standard theory for MLEs, $(\hat{\varsigma})_{n_0 \in \mathbb{N}}$ is consistent and asymptotically normally distributed. In fact, by Corollary 6.2.1 of [19],

$$\hat{\varsigma}_{n_0} \overset{n_0\to\infty}{\longrightarrow} \varsigma \quad \text{stochastically.} \tag{3.8}$$

Furthermore, by [19, Corollary 6.2.3], $(\hat{\varsigma})_{n_0}$ is asymptotically efficient (that is, optimal) and by [19, Theorem 6.2.3] (with $\mathcal{N}_{0,1}$ the standard normal distribution)

$$\sqrt{n_0 I(\varsigma)}\big(\hat{\varsigma}_{n_0} - \varsigma\big) \overset{n_0\to\infty}{\longrightarrow} \mathcal{N}_{0,1} \quad \text{in distribution.} \tag{3.9}$$

Here

$$I(\varsigma) = -\mathbb{E}[\mathcal{L}_N''(\varsigma)|N_0 = 1] = p_{L_{k_{\min}}} \sum_{l=k_{\min}}^{K-1} \left(\prod_{m=k_{\min}}^{l-1} \bar{p}_m \right) (1-\bar{p}_l) \frac{(\log(q_l))^2 \, q_l^{\varsigma}}{(1-q_l^{\varsigma})^2} \tag{3.10}$$

is the Fisher information for one sample. As we do not know the true value of ς and since we do not know $p_{L_{k_{\min}}}$, we replace $I(\varsigma)$ by

$$I_n(\varsigma) = -\frac{1}{n_0} \mathcal{L}_n''(\varsigma).$$

By the law of large numbers $I_N(\varsigma) \overset{n_0\to\infty}{\longrightarrow} I(\varsigma)$ almost surely, uniformly in ς in compact sets. Hence by (3.8), we have $I_N(\hat{\varsigma}) \overset{n_0\to\infty}{\longrightarrow} I(\varsigma)$ stochastically. Hence we use

$$\widehat{\sigma}^{\,2} := -1/\mathcal{L}_N''(\hat{\varsigma}) \tag{3.11}$$

as an estimator for the variance of $\hat{\varsigma}$ and obtain

$$\frac{\hat{\varsigma} - \varsigma}{\widehat{\sigma}} \overset{n_0\to\infty}{\longrightarrow} \mathcal{N}_{0,1} \quad \text{in distribution.} \tag{3.12}$$

Concluding, an asymptotic 95% confidence interval for ς is given by

$$\big[\hat{\varsigma} - 2\,\widehat{\sigma},\, \hat{\varsigma} + 2\,\widehat{\sigma}\big]. \tag{3.13}$$

We have performed the simulations for the exponents $\varsigma_2(1,1)$ and $\varsigma_2(2,2)$ as benchmark problems, and then did the simulations on a larger scale for

$$\varsigma_3(1,1,1), \quad \varsigma_3(1,1,2), \quad \varsigma_4(1,1,1,1), \quad \varsigma_4(1,1,1,2).$$

3.2 Two-level scheme. The simulations turn out to be very time-consuming, especially for the exponents with a larger numerical value. In order to get a more efficient scheme in this situation consider the following simplification of the simulation scheme presented above:

Assume there are only three box sizes, L_0 (about 30), L_1 (about 10 000) and $L_2 = 2L_1$. Then (3.7) can be solved explicitly and the maximum likelihood estimator for ς is

$$\hat{\varsigma} = -\frac{\log(n_2/n_1)}{\log(2)}.$$

In order to reduce the variance of $\hat{\varsigma}$ we have to increase N_1, that is the sample size n_0. However, since it takes much CPU time to obtain a sample that contributes to N_1, we may wish to use this very sample as the starting point for a number m of trials running from box size L_1 to L_2. Assume that x among these m trials have survived until L_2 (that is, have reached the boundary of the L_2-box without producing a multiple intersection), then $p_S = \frac{x}{m}$ is an estimator for the conditional probability of producing no multiple intersection until leaving the L_2-box for the given realisation S of the paths of all walks in the L_1-box. Now we can prescribe the number $n = n_1$ of "master samples" and for $i = 1, \dots, n$ let x_i be the corresponding number of surviving trials and write $\widehat{p_i} := x_i/m$. Hence for

$$p := \frac{p_{L_2}}{p_{L_1}} = \mathbb{E}[p_S]$$

we get the unbiased estimator

$$\hat{p} = \frac{1}{n}\sum_{l=1}^{n} \widehat{p_i}.$$

The unbiased estimator for the variance of $\hat{p}$ is

$$\widehat{\sigma_p^2} = \frac{1}{n(n-1)}\sum_{l=1}^{n} (\widehat{p_i} - \hat{p})^2.$$

From $\hat{p}$ and $\widehat{\sigma_p^2}$ we obtain the estimators for ς and the variance σ^2 of $\hat{\varsigma}$

$$\hat{\varsigma} = -\frac{\log(p)}{\log(2)} \qquad \text{and} \qquad \widehat{\sigma^2} = \frac{\widehat{\sigma_p^2}}{(\log(2)\,\hat{p})^2}. \tag{3.14}$$

We have employed this scheme for the exponents with numerical values larger than 2, and we explain now why it is more efficient in these cases.

The expected time planar random walk needs to go from the boundary of $\{-L, \dots, L\}^2$ to the boundary of $\{-L-1, \dots, L+1\}^2$ is of order L. The probability that a given sample ever reaches the boundary of $\{-L-1, \dots, L+1\}^2$ is of order $L^{-\varsigma}$. Hence (if we stop the simulation as soon as the first multiple intersection is detected) the expected CPU time for each sample until box size L_1 is of order

$$\sum_{L=L_0}^{L_1} L^{1-\varsigma}.$$

For $\varsigma > 2$ this sum is of order 1, for $\varsigma \leq 2$, it is of order $L_1^{2-\varsigma}$. Now the probability that a sample reaches box size L_1 without producing a multiple intersection is of order $L_1^{-\varsigma}$. Hence the expected

CPU time needed for simulating a "master sample" is of order $L^{2\vee\varsigma}$. On the other hand, each of the trials started from the master sample needs an expected CPU time of order L_1^2. Hence for $\varsigma > 2$ we can run $m = L_1^{\varsigma-2}$ trials without increasing the CPU significantly.

In order to make a good choice for m, compute the variance of $\hat{p}$

$$\mathrm{Var}[\hat{p}] = n^{-1}\mathrm{Var}[p_S] + \frac{1}{mn}\mathbb{E}[p_S(1-p_S)] \le n^{-1}\mathrm{Var}[p_S] + \frac{1}{mn}\mathbb{E}[p_S].$$

The quantities $\mathrm{Var}[p_S]$ and $\mathbb{E}[p_S] \approx 2^{-\varsigma}$ can be estimated from a test simulation as well as the expected CPU time T_1 to produce a master sample and the expected time T_2 used for each subsequent trial. Now it is an optimisation problem for the total CPU time $n(T_1 + mT_2)$ versus the variance $\mathrm{Var}[\hat{p}]$. For some of the simulations we have done test runs and solved the optimisation problem. Here $m = 1000$ turned out to be a reasonable choice that we have then used in all simulations.

We have performed the simulations according to this scheme with $L_0 = 30$, $L_1 = 10\,000$, $L_2 = 20\,000$ and $m = 1000$ for the exponents

$$\varsigma_3(1,3,3), \quad \varsigma_3(2,2,2), \quad \varsigma_3(2,2,3), \quad \varsigma_3(2,3,3), \quad \varsigma_4(2,2,2,2).$$

3.3 Numerical results. We present our estimated values $\hat{\varsigma}$ together with a statistical error of 2σ. For the systematic error it is hard to make a good judgement. From the graphical representation of the results (see below) it seems that for $\varsigma_3(1,1,2)$ the systematic error is of a smaller order than the statistical error. For $\varsigma_3(1,1,2)$ and $\varsigma_3(1,1,1)$ it is presumably of the same order. Finally, for $\varsigma_4(1,1,1,1)$ and, even worse for $\varsigma_5(1,1,1,1,1)$ we seem to systematically underestimate the values. It would require a lot larger $L_{\max}$ to get more accurate results. For that reason we have not taken too much effort to reduce the statistical error. However, we give the results of the simulations just to provide an idea of the possible values.

exponent	$\hat{\varsigma}$	$2\hat{\sigma}$	rigorous	$L_{\min}$	$L_{\max}$	$n_0/10^6$	CPU time/h
$\varsigma_2(1,1)$	1.2502	0.001	5/4	1069	20 000	500	2 064
$\varsigma_2(2,2)$	2.9188	0.0033	$\frac{35}{12} = 2.9167$	163	20 000	40 000	1 879
$\varsigma_3(1,1,1)$	1.027	0.005	[1/2, 5/4]	18 575	80 000	60	8 262
$\varsigma_3(1,1,2)$	1.2503	0.0011	[1, 5/4]	1069	80 000	200	5 858
$\varsigma_4(1,1,1,1)$	0.877	0.006	[1/4, 5/4]	39 813	80 000	20	18 262
$\varsigma_4(1,1,1,2)$	1.02	0.004	[1/2, 5/4]	27 194	40 000	200	35 212
$\varsigma_5(1,1,1,1,1)$	0.74	0.02	[1/8, 5/4]	27 194	40 000	0.74	1 147

Table 1: Numerical results obtained from the first simulation scheme.

exponent	$\hat{\varsigma}$	$2\widehat{\sigma}$	rigorous	n	CPU time/h
$\varsigma_3(1,3,3)$	2.688	0.01	$[2,\ (13+\sqrt{73})/8]$	18 100	61 860
$\varsigma_3(2,2,2)$	2.786	0.01	$[2,\ 35/12]$	16 000	47 943
$\varsigma_3(2,2,3)$	2.937	0.01	$[2,\ 35/12]$	23 000	116 888
$\varsigma_3(2,3,3)$	3.767	0.057	$[2,\ 35/12]$	1 000	179 543
$\varsigma_4(2,2,2,2)$	2.664	0.01	$[2,\ 35/12]$	16 000	63 496

Table 2: Numerical results obtained from the second simulation scheme.

3.4 Detailed Data.

3.4.1 Exponent $\varsigma_2(1,1)$.

The exact value $\varsigma_2(1,1) = 5/4$ is known. This simulation is used as a benchmark test for our simulation.

L_k	n_k	L_k	n_k	L_k	n_k	L_k	n_k	L_k	n_k
30	500000000	113	109366745	455	19660552	1890	3323382	7881	557957
33	455164209	124	97714439	500	17483797	2079	2950258	8669	495180
36	414185142	136	87320799	550	15525080	2286	2620862	9535	439662
39	379373384	149	78109962	605	13788917	2514	2327160	10488	389839
42	349383901	163	69978568	665	12253892	2765	2066024	11536	345918
46	315390855	179	62384176	731	10890052	3041	1834523	12689	307046
50	286840826	196	55800459	804	9669275	3345	1628901	13957	272420
55	257075021	215	49786852	884	8589857	3679	1446024	15352	241798
60	232385705	236	44382636	972	7631215	4046	1283655	16887	214746
66	207870728	259	39563995	1069	6776772	4450	1140213	18575	190486
72	187620511	284	35298660	1175	6020939	4895	1012659	20000	173506
79	168084821	312	31418279	1292	5347118	5384	898680		
86	151902122	343	27932867	1421	4747333	5922	797641		
94	136553134	377	24837149	1563	4214131	6514	708293		
103	122326905	414	22109889	1719	3741150	7165	628813		

Values used for the fit: $L_k = 1069 \ldots 20\,000$. CPU time 2064h.

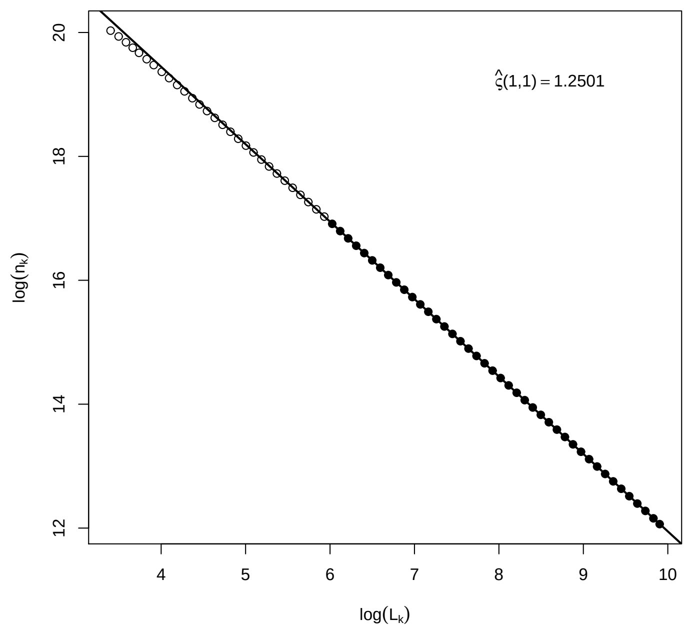

Figure 2: Linear regression for the simulation of $\varsigma_2(1,1)$.

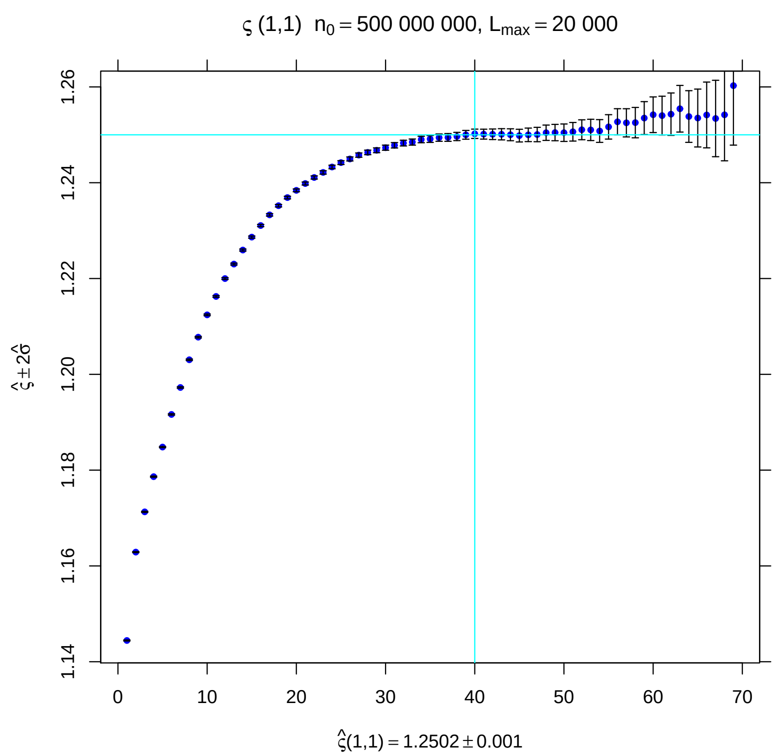

Figure 3: Simulation for $\varsigma_2(1,1)$. The co-ordinate shows $k_{\min}$, the ordinate shows the corresponding $\hat{\varsigma}$ with error bars. The vertical line indicates $k_{\min} = 40$ which we chose for our estimate of $\hat{\varsigma}$. The horizontal line shows the true value.

3.4.2 Exponent $\varsigma(2,2)$.

The exact value $\varsigma_2(2,2) = 35/12 = 2.91666\ldots$ is known. Also this simulation serves as a benchmark for our simulations.

L_k	n_k	L_k	n_k	L_k	n_k	L_k	n_k	L_k	n_k
30	40000000000	113	459313243	455	7559087	1890	117893	7881	1872
33	27956276949	124	347384944	500	5737717	2079	89442	8669	1450
36	19934507109	136	263528000	550	4343548	2286	67757	9535	1108
39	14769670878	149	200799711	605	3288311	2514	51314	10488	853
42	11270896745	163	153819037	665	2496057	2765	38803	11536	650
46	8156016609	179	116600065	731	1893876	3041	29341	12689	479
50	6108280379	196	89210485	804	1434709	3345	22363	13957	348
55	4423365460	215	67932955	884	1087314	3679	16949	15352	266
60	3315611015	236	51656232	972	823685	4046	12813	16887	193
66	2432628801	259	39313221	1069	624023	4450	9738	18575	151
72	1842369408	284	30007400	1175	473832	4895	7339	20000	123
79	1375726309	312	22780638	1292	359121	5384	5571		
86	1056545535	343	17265563	1421	271557	5922	4218		
94	803537797	377	13094893	1563	205432	6514	3229		
103	607993657	414	9961095	1719	155585	7165	2477		

Values used for the fit: $L_k = 605\ldots 20000$. CPU time 1879h.

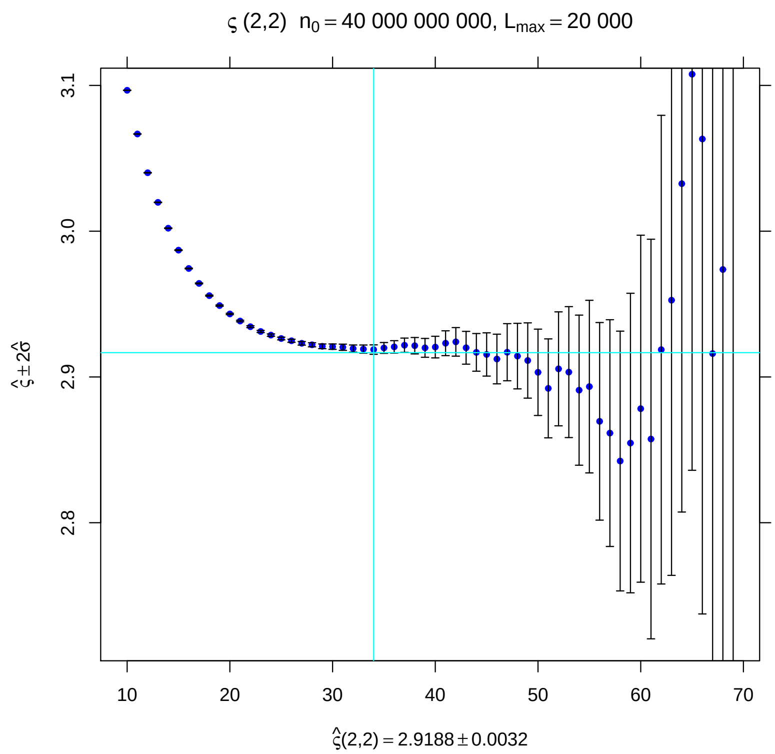

Figure 4: Simulation for $\varsigma_2(2,2)$. The co-ordinate shows $k_{\min}$, the ordinate shows the corresponding $\hat{\varsigma}$ with error bars. The vertical line indicates $k_{\min} = 34$ which we chose for our estimate of $\hat{\varsigma}$. The horizontal line shows the true value.

3.4.3 Exponent $\varsigma_3(1,1,1)$.

The exact value of $\varsigma_3(1,1,1)$ is unknown.

L_k	n_k	L_k	n_k	L_k	n_k	L_k	n_k	L_k	n_k
30	60000000	149	25859377	804	5614962	4450	1028587	24722	179046
33	59710616	163	24028791	884	5121770	4895	934379	27194	162421
36	58947709	179	22226328	972	4670981	5384	848491	29913	147273
39	57896946	196	20584233	1069	4256241	5922	770449	32904	133514
42	56673833	215	19009323	1175	3879722	6514	699523	36194	121333
46	54898618	236	17526913	1292	3534606	7165	635064	39813	109856
50	53061195	259	16147690	1421	3218775	7881	576119	43794	99544
55	50777396	284	14873454	1563	2930010	8669	523319	48173	90226
60	48570208	312	13666336	1719	2666485	9535	474777	52990	81910
66	46070175	343	12537025	1890	2426899	10488	430885	58289	74069
72	43747356	377	11494795	2079	2208165	11536	391134	64117	67148
79	41266693	414	10540910	2286	2009516	12689	354964	70528	60809
86	39014779	455	9652748	2514	1827541	13957	321882	77580	54981
94	36696389	500	8835893	2765	1661614	15352	291736	80000	53301
103	34372986	550	8076259	3041	1510468	16887	264553		
113	32097711	605	7376857	3345	1372149	18575	239803		
124	29906035	665	6740503	3679	1246493	20432	217707		
136	27820941	731	6155608	4046	1132343	22475	197364		

Values used for the fit: $L_k = 18575 \ldots 80\,000$. CPU time 8262h.

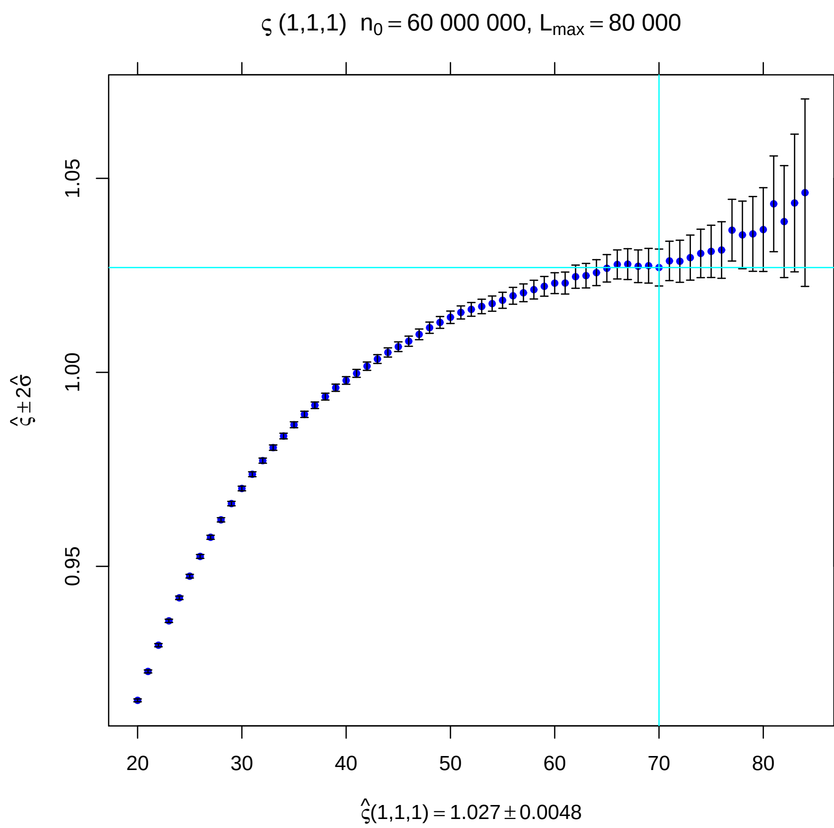

Figure 5: Simulation for $\varsigma_3(1,1,1)$. The co-ordinate shows $k_{\min}$, the ordinate shows the corresponding $\hat{\varsigma}$ with error bars. The vertical line indicates $k_{\min} = 70$ which we chose for our estimate of $\hat{\varsigma}$. The horizontal line shows the estimated value.

3.4.4 Exponent $\varsigma_3(1,1,2)$.

The exact value of $\varsigma_3(1,1,2)$ is unknown.

L_k	n_k	L_k	n_k	L_k	n_k	L_k	n_k	L_k	n_k
30	200000000	149	54585738	804	7029965	4450	826443	24722	97235
33	198136199	163	49210675	884	6245336	4895	733837	27194	86246
36	193436538	179	44119702	972	5545792	5384	651874	29913	76472
39	187242650	196	39647836	1069	4923405	5922	578486	32904	67873
42	180308394	215	35523866	1175	4374033	6514	513593	36194	60371
46	170682110	236	31776899	1292	3885012	7165	456239	39813	53674
50	161176218	259	28415711	1421	3449618	7881	405240	43794	47628
55	149901066	284	25417521	1563	3062025	8669	359523	48173	42353
60	139521065	312	22668175	1719	2718548	9535	319391	52990	37627
66	128301060	343	20191522	1890	2415286	10488	283792	58289	33387
72	118361321	377	17981958	2079	2144282	11536	251871	64117	29608
79	108205442	414	16028002	2286	1904636	12689	223767	70528	26339
86	99385254	455	14267282	2514	1690316	13957	198585	77580	23407
94	90671582	500	12694594	2765	1499756	15352	176146	80000	22541
103	82304628	550	11279842	3041	1331441	16887	156219		
113	74445095	605	10020648	3345	1181425	18575	138744		
124	67187208	665	8909164	3679	1048523	20432	123285		
136	60566796	731	7917614	4046	930691	22475	109424		

Values used for the fit: $L_k = 1069 \ldots 10\,000$. CPU time 5858h.

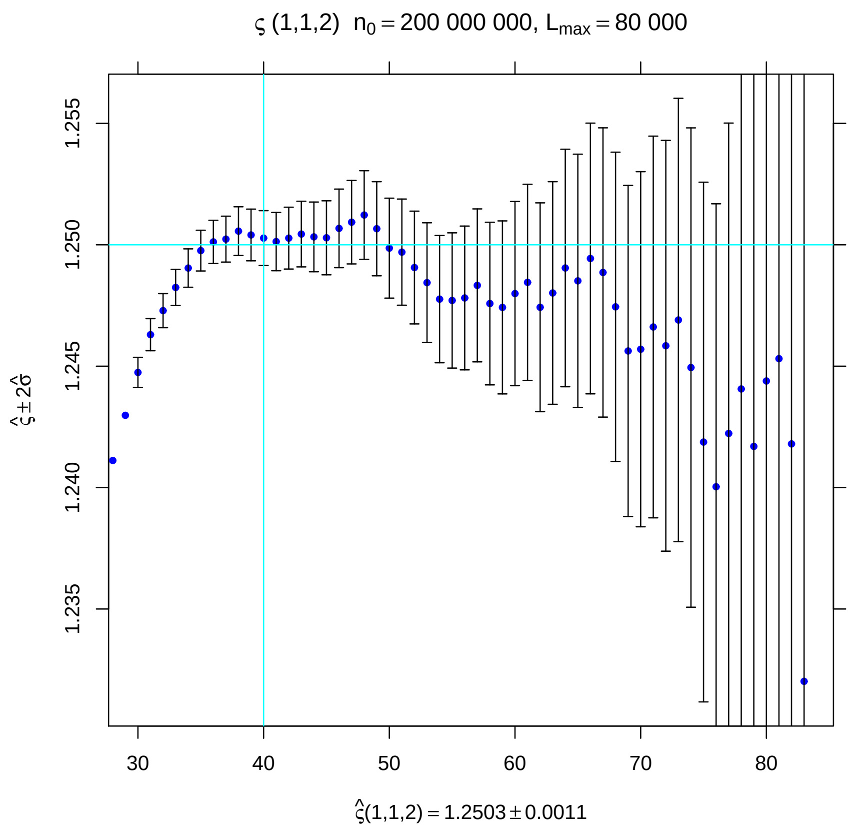

Figure 6: Simulation for $\varsigma_3(1,1,2)$. The co-ordinate shows $k_{\min}$, the ordinate shows the corresponding $\hat{\varsigma}$ with error bars. The vertical line indicates $k_{\min} = 40$ which we chose for our estimate of $\hat{\varsigma}$. The horizontal line shows the conjectured value $\varsigma_3(1,1,2) = \varsigma_2(1,1) = 5/4$.

3.4.5 Exponent $\varsigma_4(1,1,1,2)$.

The exact value of $\varsigma_4(1,1,1,2)$ is unknown.

L_k	n_k	L_k	n_k	L_k	n_k	L_k	n_k	L_k	n_k
30	200000000	124	126992806	550	38132997	2514	8950110	11536	1953289
33	199921620	136	119464557	605	34954676	2765	8149013	12689	1773558
36	199482984	149	112181604	665	32040238	3041	7419539	13957	1609927
39	198565228	163	105219661	731	29348812	3345	6752347	15352	1461067
42	197176986	179	98203442	804	26850724	3679	6144676	16887	1326172
46	194683952	196	91672706	884	24560465	4046	5589138	18575	1203707
50	191624492	215	85304312	972	22451887	4450	5082774	20432	1092672
55	187237710	236	79199999	1069	20511329	4895	4621823	22475	991657
60	182471375	259	73434697	1175	18739197	5384	4201858	24722	900187
66	176514402	284	68044645	1292	17110256	5922	3819442	27194	816464
72	170515344	312	62863201	1421	15612645	6514	3470994	29913	740704
79	163642608	343	57973159	1563	14238301	7165	3155561	32904	672302
86	157023575	377	53412940	1719	12983348	7881	2866913	36194	609756
94	149860203	414	49196512	1890	11838167	8669	2604947	39813	553485
103	142343356	455	45240841	2079	10786022	9535	2366048	40000	550828
113	134666159	500	41572496	2286	9827571	10488	2149715		

Values used for the fit: $L_k = 27\,194, \ldots, 40\,000$. CPU time 35 212h.

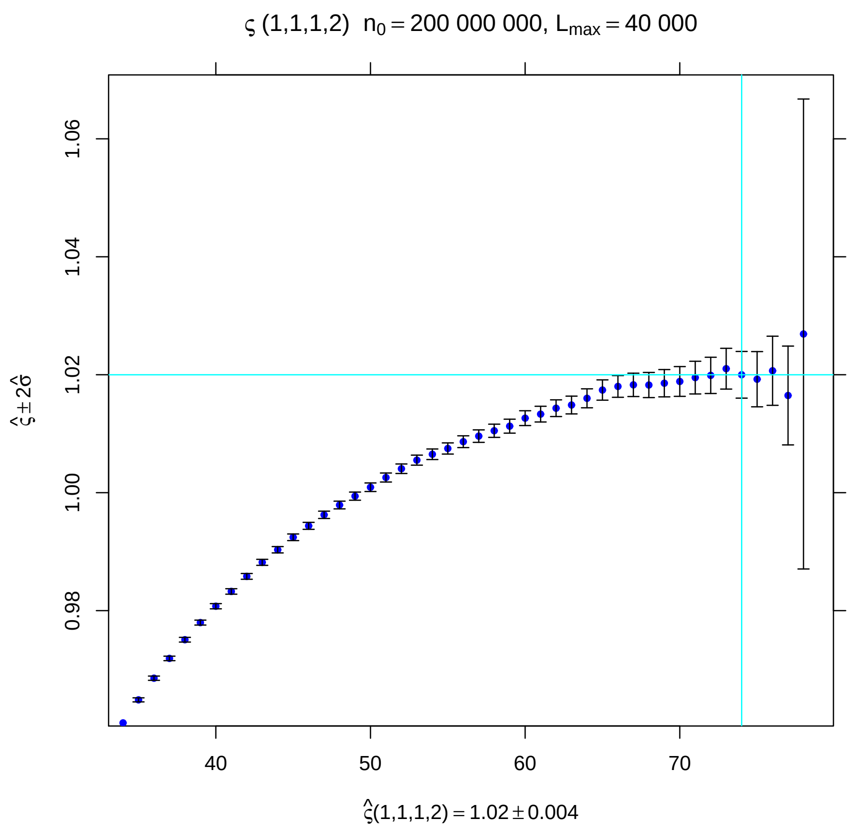

Figure 7: Simulation for $\varsigma_4(1,1,1,2)$. The co-ordinate shows k_{min}, the ordinate shows the corresponding $\hat{\varsigma}$ with error bars. The vertical line indicates $k_{\text{min}} = 74$ which we chose for our estimate of $\hat{\varsigma}$. The horizontal line shows the estimated value.

3.4.6 Exponent $\varsigma_4(1,1,1,1)$.

The exact value of $\varsigma_4(1,1,1,1)$ is unknown.

L_k	n_k
30	20000000
33	19996035
36	19972855
39	19923361
42	19846358
46	19704559
50	19524417
55	19258012
60	18958581
66	18573948
72	18172653
79	17698995
86	17228707
94	16704112
103	16136193
113	15537061
124	14922694
136	14299200

L_k	n_k
149	13677483
163	13066040
179	12433477
196	11828110
215	11220785
236	10622843
259	10040743
284	9483483
312	8935078
343	8402393
377	7892203
414	7410458
455	6946326
500	6504855
550	6081417
605	5681289
665	5304532
731	4949662

L_k	n_k
804	4613179
884	4297577
972	4001670
1069	3722426
1175	3461745
1292	3217081
1421	2987877
1563	2773980
1719	2573328
1890	2386906
2079	2213006
2286	2051046
2514	1899964
2765	1758768
3041	1628269
3345	1506688
3679	1393480
4046	1289159

L_k	n_k
4450	1191616
4895	1101052
5384	1017194
5922	939586
6514	867259
7165	801006
7881	739646
8669	682392
9535	629677
10488	580582
11536	535316
12689	493266
13957	454757
15352	419131
16887	386266
18575	356146
20432	328229
22475	302420

L_k	n_k
24722	278878
27194	256535
29913	236157
32904	217434
36194	200369
39813	184289
43794	169567
48173	156118
52990	143655
58289	132091
64117	121391
70528	111643
77580	102601
80000	99860

Values used for the fit: $L_k = 39\,813 \ldots 80\,000$. CPU time 18 262h.

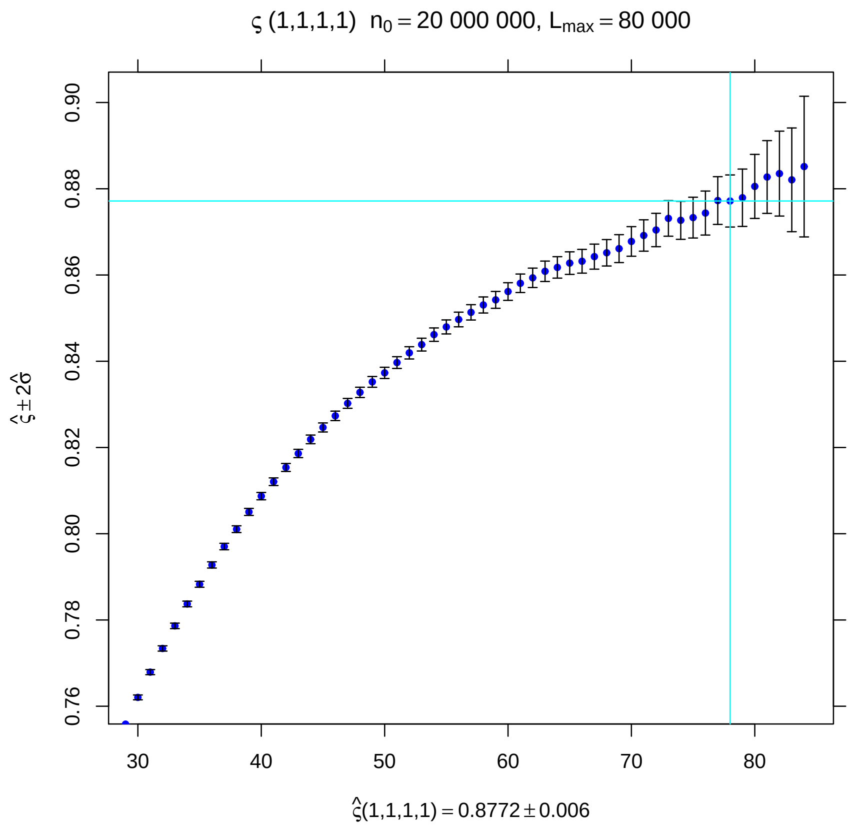

Figure 8: Simulation for $\varsigma_4(1,1,1,1)$. The co-ordinate shows k_{min}, the ordinate shows the corresponding $\hat{\varsigma}$ with error bars. The vertical line indicates $k_{\text{min}} = 78$ which we chose for our estimate of $\hat{\varsigma}$. The horizontal line shows the estimated value.

3.4.7 Exponent $\varsigma_5(1,1,1,1,1)$.

The exact value of $\varsigma_5(1,1,1,1,1)$ is unknown.

L_k	n_k
30	744165
33	744158
36	744107
39	743886
42	743487
46	742538
50	741155
55	738765
60	735484
66	730711
72	725183
79	718008
86	710226
94	700782
103	689769
113	677384

L_k	n_k
124	663493
136	648801
149	633473
163	617246
179	599664
196	581885
215	562961
236	543820
259	524462
284	505282
312	485535
343	465955
377	446300
414	426779
455	407418
500	388692

L_k	n_k
550	370165
605	352289
665	335283
731	318821
804	302365
884	286416
972	271268
1069	256593
1175	242487
1292	229014
1421	216285
1563	204002
1719	192310
1890	181055
2079	170456
2286	160399

L_k	n_k
2514	150828
2765	141592
3041	133025
3345	124845
3679	117257
4046	109961
4450	102996
4895	96520
5384	90434
5922	84699
6514	79371
7165	74357
7881	69601
8669	65234
9535	61002
10488	56977

L_k	n_k
11536	53144
12689	49724
13957	46458
15352	43355
16887	40574
18575	37983
20432	35448
22475	33083
24722	30843
27194	28666
29913	26699
32904	24955
36194	23207
39813	21616
40000	21535

Values used for the fit: $L_k = 27\,194 \ldots 40\,000$. CPU time 1147h.

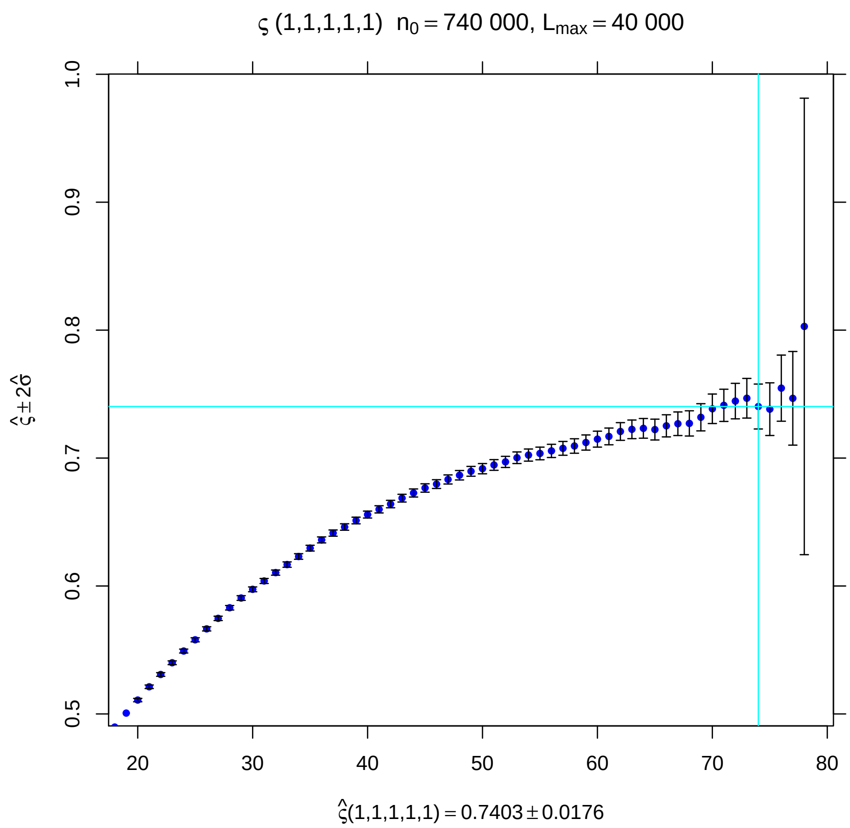

Figure 9: Simulation for $\varsigma_5(1,1,1,1,1)$. The co-ordinate shows $k_{\min}$, the ordinate shows the corresponding $\hat{\varsigma}$ with error bars. The vertical line indicates $k_{\min} = 74$ which we chose for our estimate of $\hat{\varsigma}$. The horizontal line shows the estimated value.

3.4.8 Exponent $\varsigma_3(1,3,3)$.

The exact value of $\varsigma_3(1,3,3)$ is unknown. As it turns out that $\varsigma_3(1,3,3) > 2$, we have performed simulations according to our scheme 2. That is, we have generated n master samples of random walk paths that reach the boundary of the L_1-box (here $L_1 = 10000$). For each such master sample i we have run $m = 1000$ trials and have counted the fraction $\hat{p}_i$ of trials where the paths reached the boundary of the L_2-box (with $L_2 = 2L_1$). As $n = 18\,100$ we cannot give the complete data set $p_1, \ldots, p_n$ but rather give the empirical mean and the standard deviation of $\hat{p}$

$$\hat{p} = 0.155202983425414, \qquad \hat{\sigma}_p = 0.000536918044881792.$$

From this we compute

$$\hat{\varsigma}_3(1,3,3) = 2.6877718045551$$

with standard deviation

$$\hat{\sigma} = 0.00499094143436367.$$

We conjecture that

$$\varsigma_3(1,3,3) = \varsigma_2(1,3) = \frac{13+\sqrt{73}}{8} = 2.693000\ldots$$

We conclude with a histogram of the values p_i:

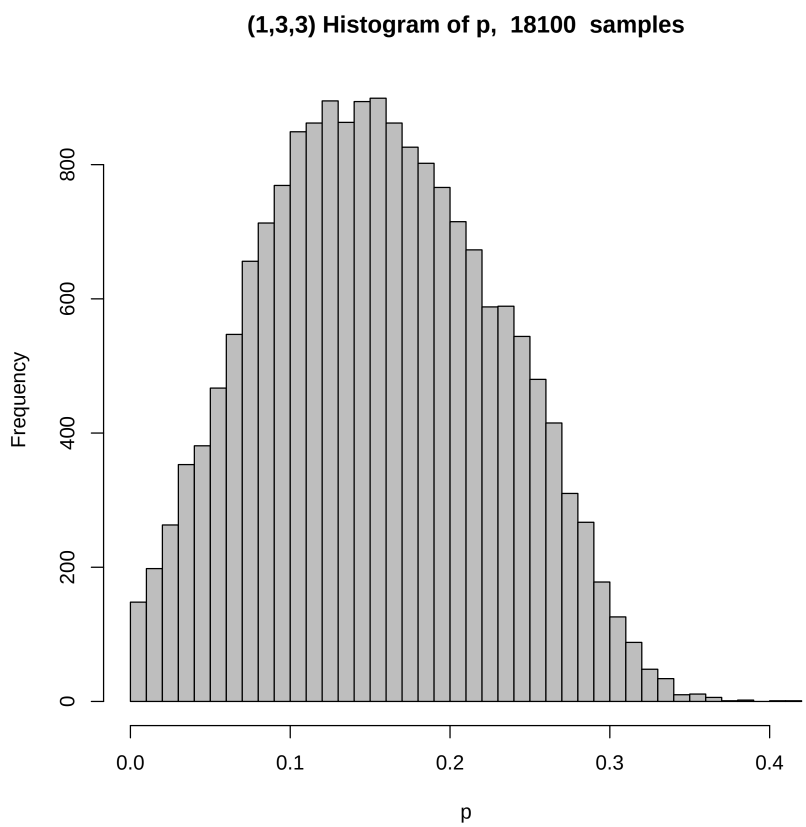

Figure 10: Histogram of the values p_i for $\varsigma_3(1,3,3)$.

3.4.9 Exponent $\varsigma_3(2,2,2)$.

The exact value of $\varsigma_3(2,2,2)$ is unknown. We have performed a simulation with the second scheme with $N = 16000$, $n = 1000$, $L_1 = 10000$, $L_2 = 20000$. Mean and standard deviation are

$$\hat{p} = 0.1449495, \qquad \hat{\sigma}_p = 0.000497221297799643.$$

From this we compute

$$\hat{\varsigma}_3(2,2,2) = 2.78637773802317$$

with standard deviation

$$\hat{\sigma} = 0.00494888703003405.$$

3.4.10 Exponent $\varsigma_3(2,2,3)$.

The exact value of $\varsigma_3(2,2,3)$ is unknown. We conjecture

$$\varsigma_3(2,2,3) = \varsigma_2(2,2) = \frac{35}{12} = 2.916666\ldots$$

We have performed a simulation with the second scheme with $N = 23000$, $n = 1000$, $L_1 = 10000$, $L_2 = 20000$. Mean and standard deviation are

$$\hat{p} = 0.130559, \qquad \hat{\sigma}_p = 0.000444444142417374.$$

From this we compute

$$\hat{\varsigma}_3(2,2,3) = 2.93722618256156$$

with standard deviation

$$\hat{\sigma} = 0.00491116935805033.$$

3.4.11 Exponent $\varsigma_3(2,3,3)$.

The exact value of $\varsigma_3(2,3,3)$ is unknown. We conjecture

$$\varsigma_3(2,3,3) = \varsigma_2(2,3) = \frac{47 + 5\sqrt{73}}{24} = 3.738334113\ldots$$

We have performed a simulation with the second scheme with $N = 1000$, $n = 1000$, $L_1 = 10000$, $L_2 = 20000$. Mean and standard deviation are

$$\hat{p} = 0.073458, \qquad \hat{\sigma}_p = 0.00144828442088002.$$

From this we compute

$$\hat{\varsigma}_3(2,3,3) = 3.76693657262376$$

with standard deviation

$$\hat{\sigma} = 0.0284439101500224.$$

This simulation was particularly time consuming (179 543h CPU time) as the actual value of $\varsigma_3(2,3,3)$ is rather large and it thus takes a tremendous amount of time to generate each master sample.

3.4.12 Exponent $\varsigma_4(2,2,2,2)$.

The exact value of $\varsigma_4(2,2,2,2)$ is unknown. We have performed a simulation with the second scheme with $N = 16000$, $n = 1000$, $L_1 = 10000$, $L_2 = 20000$. Mean and standard deviation are

$$\hat{p} = 0.157732125, \qquad \hat{\sigma}_p = 0.000521232849038418.$$

From this we compute

$$\hat{\varsigma}_4(2,2,2,2) = 2.66445157389522$$

with standard deviation

$$\hat{\sigma} = 0.00476745017196814.$$

Acknowledgments: P.M. is supported by the *Engineering and Physical Sciences Research Council (EPSRC)* through an Advanced Research Fellowship.

Bibliography

[1] K. Burdzy, G. Lawler and T. Polaski. On the critical exponent for random walk intersections. *J. Statist. Phys.* 56, 1-12 (1989).

[2] F. Camia and C. M. Newman. Two-dimensional critical percolation: the full scaling limit. *Comm. Math. Phys.*, 268, 1–38 (2006).

[3] F. Camia and C. M. Newman. Critical percolation exploration path and SLE_6: a proof of convergence. *Probab. Theory Related Fields* 139, 473–519 (2007).

[4] J. Cardy. Critical percolation in finite geometries. *J. Phys. A*, 25, L201-L206 (1992).

[5] B. Duplantier. Random walks and quantum gravity in two dimensions. *Phys. Rev. Lett.*, 81, 5489-5492 (1998).

[6] B. Duplantier and K.-H. Kwon. Conformal invariance and intersections of random walks. *Phys. Rev. Lett.*, 61, 2514-2517 (1988).

[7] B. Duplantier and S. Sheffield. Duality and the Knizhnik-Polyakov-Zamolodchikov Relation in Liouville Quantum Gravity. *Phys. Rev. Lett.* 102, 150603 (2009).

[8] A. Klenke and P. Mörters. The multifractal spectrum of Brownian intersection local time. *Ann. Probab.* 33, 1255-1301 (2005).

[9] D. E. Knuth. The art of computer programming. Vol. 2, 3rd edition. Addison-Wesley, Boston MA (2005).

[10] G. F. Lawler. Intersections of random walks with random sets. *Israel J. Math.* 65, 113-132 (1989).

[11] G. F. Lawler. Intersections of random walks. Birkhäuser, Boston MA (1991).

[12] G. F. Lawler. Nonintersecting planar Brownian motions. *Math. Phys. El. Journal*, 1, Paper 4, pp 1-35 (1995).

[13] G. F. Lawler. Hausdorff dimension of cut points for Brownian motion. *El. Journal Probab.*, 1, Paper 2, pp 1-20 (1996).

[14] G. F. Lawler, O. Schramm and W. Werner. Values of Brownian intersection exponents I: Half-plane exponents. *Acta Math.*, 187, 237-273 (2001).

[15] G. F. Lawler, O. Schramm and W. Werner. Values of Brownian intersection exponents II: Plane exponents. *Acta Math.*, 187 , 275–308 (2001).

[16] G. F. Lawler, O. Schramm and W. Werner. Values of Brownian intersection exponents III: Two-sided exponents. *Ann. Inst. Henri Poincaré*, 38, 109-123 (2002).

[17] G. F. Lawler, O. Schramm and W. Werner. Analyticity of intersection exponents for planar Brownian motion. *Acta Math.* 189, 179–201 (2002).

[18] P. L. Leath and G R Reich. Scaling form for percolation cluster sizes and perimeters. *J. Phys. C* 11, 4017–4036 (1978).

[19] E. L. LEHMANN. Theory of point estimation. *Wiley, New York* (1983).

[20] B. LI and A. SOKAL. High-precision Monte Carlo test of the conformal-invariance predictions for two-dimensional mutually avoiding walks. *J. Statist. Phys.* 61, 723–748 (1990).

[21] P. MÖRTERS and Y.PERES. Brownian motion. *Cambridge University Press* (2009).

[22] P. MÖRTERS and N.-R. SHIEH. The exact packing measure of Brownian double points. *Probab. Theory Related Fields* 143, 113–136 (2009).

[23] R. RHODES and V. VARGAS. KPZ formula for log-infinitely divisible multifractal random measures. arXiv:0807.1036 (July 2008).

[24] B. SALEUR and B. DUPLANTIER. Exact determination of the percolation hull exponent in two dimensions. *Phys. Rev. Lett.*, 58, 2325 - 2328 (1987).

[25] S. SMIRNOV. Critical percolation in the plane: conformal invariance, Cardy's formula, scaling limits. *C. R. Acad. Sci. Paris Sr. I Math.* 333, 239–244 (2001).

[26] R.F. VOSS. The fractal dimension of percolation cluster hulls. *J. Phys. A* 17, L373-L377 (1984).